SPECTRA FOR EARTHQUAKE RESISTIVE DESIGN OF UNDERGROUND LONG STRUCTURES

by

Yoshinori AOKI* and Satoshi HAYASHI**

SYNOPSIS

Two methods for the earthquake resistive design of subaqueous tunnels have been examined, that is, the spectra method and the response analysis using the electronic computer. This paper describes the calculation process based on the spectra method and proposes spectra patterns necessary for design calculation.

Strong motion earthquake records at port and harbour facilities have been installed from the strong motion earthquake observation network at the Port and Harbour Research Institute. Among those records 49 components, maximum acceleration of which was larger than 50 gal, were rearranged due to newly developed calculation method and were summarized into period and displacement amplitude of equivalent sinusoidal wave. Standard spectra for design calculation was shown according to three grades (A, B' and C') classified from 49 components, as was deduced from the standpoint of relationship between foundation of observation area and magnitude of earthquake.

INTRODUCTION

Possible damages of long underground structures such as tunnels constructed by the trench method may be caused by those occasions which can be classified into following three categories; the 1 st, the structure happens to be located across an active tectonic fault, then the structure may be damaged due to its activities as a result or effect of an earthquake. The 2 nd, the structure is constructed in the site where some geological defects exist, then the structure may be damaged due to liquefaction of the foundation or backfill material, or due to failure of the surrounding soft soil. The 3 rd, stresses induced in the structure due to dynamic deformation of the surrounding soil during an earthquake exceed the strength of structural material. This paper discusses only problems in the field of the last category.

Research works concerned with the earthquake resistive design method of trench type tunnels have been done mainly from the following three aspects; the 1 st is the dynamic model test. The research done by Tamura et al.[1] has made the model test practical. The 2 nd is the

* Former Chief, Materials Laboratory, Structures Division, Port and Harbour Research Institute, Ministry of Transport, Japanese Government

** Head, Structures Division, Port and Harbour Research Institute.

response snalysis by using an electronic computer. [2),3),4)] The last is the design method using design spectra. The development of a new design method [5)] which the BART tunnel project was accompanied with is quite noteworthy. This design method is rather of practice, and has had a great influence on the practical design in Japan so far. Though researches utilizing the earthquake swarm at Matsushiro done by Sakurai et al. [6)] are not directly connected with tunnels but with underground pipelines, those are quite similar to the tunnel in some sense from the earthquake resistive design point of view and results of the researches are very suggestive.

PRINCIPLE OF THE DESIGN METHOD USING SPECTRA

This design method is based on the assumptions that underground light structures like trench type tunnels rarely resonate with earthquakes and displacement of the structure during an earthquake is at most equal to the displacement of the surrounding ground. And a displacement transfer ratio from soil to the structure depends on the rigidities of soil and the structure. Therefore if the displacement distribution of the ground during an earthquake and the displacement transfer ratio are known, the shape of deformation of the structure during the earthquake is obtained and the earthquake resistive structure, then, can be designed.

Preconditions of the computation method of the design spectra are as follows;

(1) No failure of the surrounding soil or no fault activities will be considered on the assumption that enough attentions have already been paid when the route of the tunnel is chosed.
(2) The spectra are computed from the strong motion accelerogram which is assumed to be a record of an imaginary wave propagating horizontally with an arbitrary constant velocity.
(3) The displacement transfer ratio can be calculated by treating statically the tunnel as a beam in an elastic medium.

Authors [7)] have done a field vibration model test of tunnel. According to the test result, of which an example is shown in Fig. 1, though a resonant phenomenon was observed, it was because the frequency of the excitation vibration was very high, and prototype tunnels will scarecely resonate with earthquakes, considering similitude. And also it was found that the response of the model to the shear wave propagating horizontally can be explained by assuming the model as a beam in an elastic medium and by static calculation, as is shown in Fig. 1.

COMPUTATION OF DESIGN SPECTRA

From the theory of elasticity, following basic equation is obtained, taking the tunnel axis for x-axis.

$$EI \frac{d^4 u_t}{d x^4} = K (u - u_t) \tag{1}$$

where EI, K, u and u_t stand for the bending rigidity of the tunnel, the spring constant of the soil, displacement of the soil in the transverse direction of x-axis and the displacement of the tunnel in the same direction as the soil. Taking sinusoidal waves of amplitude of U and U_t for the displacement of the soil and the tunnel respectively, that is, $u = U \sin 2\pi x/L$ and $u_t = U_t \sin 2\pi x/L$, and substituting into eq. (1), the displacement of the tunnel without boundary is obtained as follows;

$$u_t = \frac{u}{\frac{EI}{K}(\frac{2\pi}{L})^4 + 1} = \frac{U}{\frac{EI}{K}(\frac{2\pi}{L})^4 + 1} \sin\frac{2\pi}{L} x \tag{2}$$

where L is the wave length of the ground displacement. Supposing the ground displacement wave propagates with a velocity of V_s, the wave length, L can be replaced by $V_s T$ and x by $V_s t$, where T is the period of the propagating ground displacement wave and t is time. Substituting these relation into eq. (2), eq. (3) is obtained.

$$u_t = \frac{U}{\frac{EI}{K}(\frac{2\pi}{V_s})^4 \frac{1}{T^4} + 1} \sin\frac{2\pi}{T} t \tag{3}$$

Introducing the following quantity

$$\tau = \frac{2\pi}{V_s} \sqrt[4]{\frac{EI}{K}} \tag{4}$$

let us call it "rigidity ratio period". This value, τ is unique for a tunnel and depends upon the rigidity of the tunnel and soil, and has a dimension of time and indicates a characteristic of the tunnel like natural period of a system. Using eq. (4), eq. (3) can be reduced as eq. (5).

$$u_t = G(\tau, T) \cdot u = \frac{U}{(\tau/T)^4 + 1} \sin\frac{2\pi}{T} t \tag{5}$$

where $G(\tau, T) = 1/(\tau^4/T^4 + 1)$ is a transfer function of the displacement from the ground to the tunnel, which depends on the rigidity ratio period and the period of the wave propagating in the ground.

The curvature, ρ of the tunnel which is deformed into the sinusoidal shape can be represented as follows;

$$\rho = \frac{d^2 u_t}{dx^2} = \frac{1}{V_s^2} \frac{d^2 u_t}{dt^2} = -G(\tau,T)\, U(\frac{2\pi}{T})^2 \frac{1}{V_s^2} \sin\frac{2\pi}{T} t \tag{6}$$

The relation between amplitudes of the displacement, U, and the acceleration, a, of a sinusoidal wave is $a=(2\pi/T)^2 U$, then eq. (6) can also be rewritten as eq. (7).

$$\rho V_s^2 = - G(\tau, T) \cdot a \cdot \sin 2\pi\, t/T \tag{7}$$

On the other hand, an accelerogram of an earthquake can be represented in a Fourier series, as follows;

$$a_e(t) = \sum_n a_n \sin\{(2\pi t/Tn) + \phi_n\} \tag{8}$$

where $a_e(t)$ is the acceleration of the earthquake, ϕ_n is the phase angle and suffix n stands for the nth term of the series. Because eq. (7) can

be applicable for each component of the Fourier amplitude represented by eq. (8), the curvature induced in a tunnel by an earthquake can be formulated as eq. (9).

$$\rho V^2_s = - \Sigma G\ (\tau, T_n) \cdot a_n \cdot \sin\ (\frac{2\pi}{T_n} t + \phi_n) \qquad (9)$$

Eq. (9) can easily be computed by an electronic computer for a digitized accelerogram and for various value of τ. Computing process is shown in Fig. 2. The top row shows the N-S component of the El Centro earthquake for first 10 seconds. The wave in the 2nd row is the repoduced wave by such a way that the original wave is expanded into a Fourier series in the range of 0.15 - 10 seconds of period then the components are again superimposed taking the phase angle into consideration. Two waves, original and reproduced coincide fairly good. Each row below the 2nd row shows the computation results of eq. (9) for τ = 0.33, 0.53, 1.16, 2.76 and 5.55 seconds in turn.

The maximum value can be taken of each wave lower than the 2nd row of Fig. 2. Repeating this process for many various value of τ, a design spectrum can be obtained for bending of a tunnel as a function of the rigidity ratio period, τ. Letting $H\rho(\tau)$ be the spectrum obtained by above process, eq. (10) is obtained.

$$H\rho\ (\tau) = |\rho V^2_s|_{max} = |\Sigma G(\tau, T_n) \cdot a_n \cdot \sin(\frac{2\pi t}{T_n} + \phi_n)\ |_{max} \qquad (10)$$

Let us call $H\rho(\tau)$ the "curvature response spectrum". $H\rho(\tau)$ has a dimension of acceleration. Fig. 3 shows the curvature response spectrum of the N-S component of the El Centro earthquake modified to 100 gal. of the maximum acceleration.

Recalling that eq. (6) gives us the curvature induced in the tunnel by a single sinusoidal wave, the relationship between the displacement amplitude and the period which gives us the same maximum curvature induced as that calculated from the earthquake can be obtained by substituting eq. (6) into eq. (10).

$$U = \frac{|\rho V^2_s|_{max}}{G(\tau, T)} (\frac{T}{2\pi})^2 = \frac{H\rho(\tau)}{G(\tau, T)} (\frac{T}{2\pi})^2 \qquad (11)$$

Eq. (11) represents a group of curves which are concave upqards on the U-T coordinate as shown in Fig.4. Taking a curve for a particular value of τ, U and T on every points along the curve gives us the same curvature induced in the tunnel which is the maximum calculated from the earthquake the curve has been computed from. An envelope of the group of the curves can be drawn as shown in Fig. 4. This envelope can be used as the design displacement spectrum for curvature. Let us call the envelope the "Displacement amplitude spectrum of equivalent sinusoidal wave for curvature", which is a function of only the period of the ground motion, T.

On Fig. 5, displacement amplitude spectrum of equivalent sinusoidal wave for curvature of the N-S component of the El Centro earthquake is shown.

Bending problems of the tunnel have been discussed so far and corresponding spectra have been led with examples illustrated. By the same manner, spectra for the shear force, the load in the transverse direction to the tunnel axis, axial strain and axial load can be obtained.

On Figs. 6∿8, the shear response spectrum, the axial strain response spectrum and the axial load response spectrum of the N-S component of the El Centro earthquake are shown. On Fig. 9, five displacement amplitude spectra of equivalent sinusoidal wave are shown. From the practical point of view, the group of curves seems to be represented by a single curve, because the group of spectra are plotted in a narrow range.

STANDARD RESPONSE SPECTRUM

Total number of strong motion earthquake records rearranged in this paper was from 13 areas, 27 records and 49 components,[8] maximum acceleration of which was larger than 50 gal. Record names of observation areas and components dealt with were shown in Table 1. Calculation was carried out regarding principal motion indicated in Table 1.

Patterns of spectra greatly depend on each observed record. Some researchers[9] reported about acceleration response spectra rearranged and classified accordingly to foundation conditions of observation sites. Observed records were also tried to be classified in this paper.

In the previous chapter, spectra calculation equations was induced. Through this process were described the response spectra and the amplitude spectrum of equivalent sinusoidal wave pertaining to five items. It may be effective approach to combine these spectra data, since various varieties of spectra needed laborious work for rearrangement and were likely to lead to confusion at the stage of practical usage. And, whole spectra were combined as the indexes of the amplitude spectrum of equivalent sinusoidal wave regarding each item, which had the dimension of frequency and displacement. The previous chapter showed from the example of El Centro (N-S) that each of five amplitude apectra of equivalent sinusoidal wave came to similar data.

On the discussion examined above, it was tried in this paper that the standard design spectra was arranged based on the classification of the amplitude spectrum of equivalent sinusoidal wave. The amplitude spectrum of equivalent sinusoidal wave on bending curvature was representatively evaluated among five kinds of spectra, Table 1 showed bending curvature spectrum data $H_\rho(1)$ at one second of rigidity ratio which was the axis of abscissa in the figure of bending curvature response spectrum. $H_\rho(1)$ was adopted as one index of spectra pattern. $H_\rho(1)$ varied from more than 50 cm/sec^2 to less than 4 cm/sec^2 as shown in Table 1. Since

these spectrum data normalized various number of acceleration into maximum acceleration of 100 gals, it seemed that the factor regarding scale of acceleration was precluded and spectra expressed the property of original records. Moreover rearranged data stood in limited extent though some variety occurred among each earthquake record even at one observation site. Then it may sound reasonable approach to classify these data recorded only at the observation site of strong motion earthquake. 10 cm/sec^2 of $H\rho(1)$ is represented as A class, 10∿40 cm/sec^2 as B class and more than 40 cm/sec^2 as C class, respectively. Classi fication result was described in Table 1. However, $H\rho(1)$ showed comparatively large value in the case of earthquake of large magnitude recorded at such places as Ofunado and Hachinohe. This fact may lead to the presumption that $H\rho(1)$ was influenced by magnitude of earthquake. Foundation condition of class A was considerably tightened sand layer or sandy gravel layer corresponding to N value of more than 50, and that of class C was loose sand layer corresponding to N value of less than 5 or deep soft clay layer. Medium foundation condition belonging to neither two categories mentioned above was corresponding to class B.

It may be presumed that larger value of $H\rho(1)$ came out under the condition of such two combined factors as soft ground and large magnitude of earthquake. Records having larger magnitude of earthquake and $H\rho(1)$ at Hachinohe and Ofunado were picked up among classified data shown above and were denoted as class C'. In the case of data in which $H\rho(1)$ was small (magnitude also showed small) at Aomori, class B was replaced into class B' (see the 3rd column of Table 1). Figs. 10 to 12 showed average of amplitude spectra which was represented with the amplitude apectra of equivalent sinusoidal wave corresponding to bending curvature of three classes. Range of 1σ (standard deviation) and 2σ were added in Figs. 10 to 12. Each line indicated average 1σ and 2σ from lower part of each figure. Figs. 13 to 15 showed average value, average plus 1σ and average plus 2σ as standard spectra precluding original data.

CONCLUDING REMARKS

Calculation equation was induced regarding spectra for earthquake resistive design of subaqueous tunnels. 49 records of horizontal components observed at 13 sites were provided for the purpose of spectra calculation. These design spectra, which were represented with the displacement spectra of equivalent sinusoidal wave, were classified according to observation sites of strong motion earthquake records and magnitude of earthquake, After the calculation of average and dispersion, spectra of class A, B' and C' were proposed as standard spectra of each class.

REFERENCES

1) C. Tamura and T. Okazaki: Dynamic Model Test of Trench Type Tunnel, Preprint of 11 th Earthquake Engineering Symposium on Civil Engineering Structure, pp 29-32, July, 1971

2) K. Muto, K. Uchida and T. Tsugawa: The Earthquake Response Analysis of Underground Tunnels, Proc., 3 rd Japan Earthquake Engineering Symposium, pp 437-444, Nov., 1970

3) M. Hamada: Earthquake Response Analysis of Trench Type Tunnels, Preprint of 26 th Annual Conference of JSCE, pp 317-320, Oct. 1971

4) Y. Goto, J. Ohta and T. Sato: Earthquake Analysis of Trench Type Tunnels by F. E. M., Preprint of 26 th Annual Conference of JSCE, pp 321-324, Oct., 1971

5) The San Francisco Bay Area Rapid Transit Commission; Technical Supplement to the Engineering Report, 1960, July. (Translated in Japanese by the Public Works Research Institute, 1968 Oct.)

6) A. Sakurai: Earthquake Resistivity of Underground Pipelines, Preprint of Regional Symposium of JSSMFE, Hokkaido Branch, Oct., 1970

7) Y. Aoki, H. Tsuchida and S. Hayashi: Outdoor Dynamic Model Test of Trench Type Tunnel, Preprint of 11 th Earthquake Engineering Symposium on Civil Engineering Structures, pp 21-24, July, 1971

8) H. Tsuchida, et al., Annual Report on Strong-Motion Earthquake Records In Japanese Ports, Technical Note of The Port and Harbour Research Institute, No. 55, 62, 64, 98, 100, 116 and 136.

9) S. Hayashi, et al., Acceleration Response Spectra on Various Site Condition, Proc. of the 3rd Japan Earthquake Engineering Symposium, pp 207-214, Nov., 1970

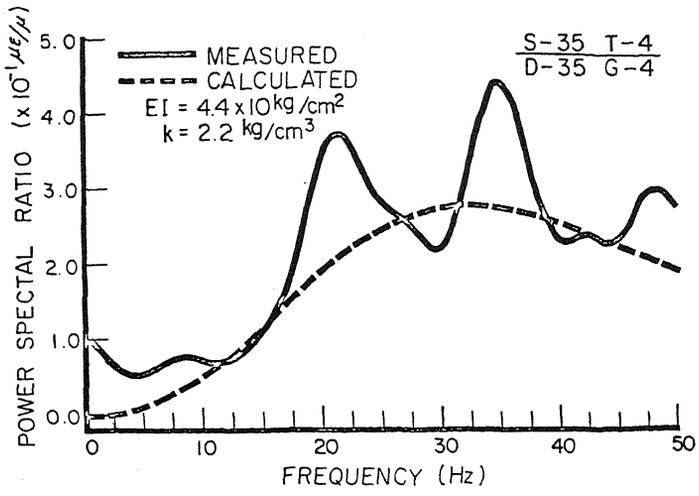

FIG. 1 RESULT OF DYNAMIC MODEL TEST

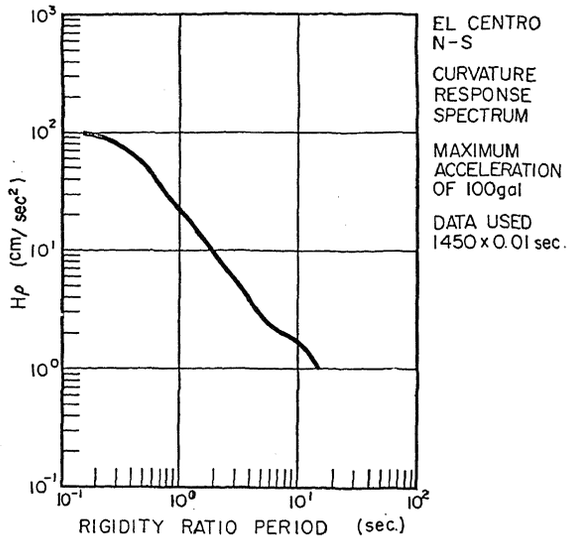

FIG. 3 CURVATURE RESPONSE SPECTRUM

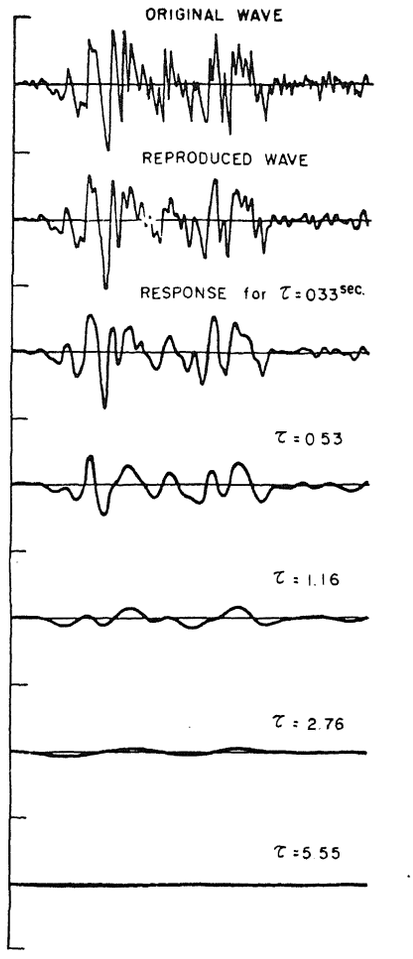

FIG. 2 COMPUTING PROCESS OF DESIGN SPECTRUM

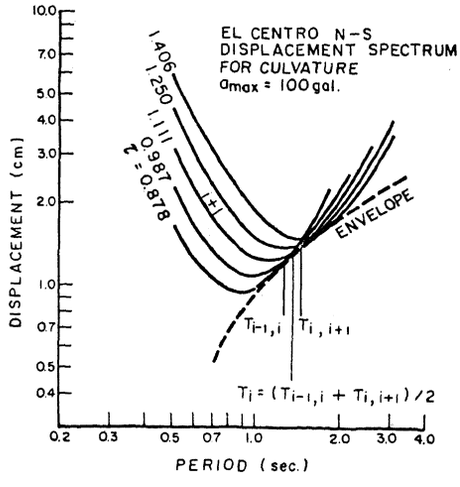

FIG. 4 RELATION BETWEEN DISPLACEMENT & PERIOD

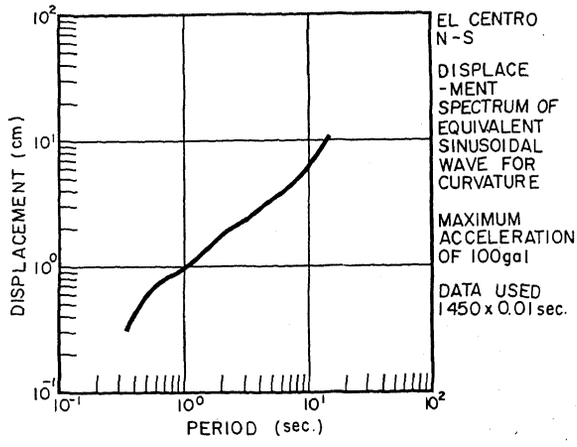

FIG. 5 DISPLACEMENT SPECTRUM FOR CURVATURE

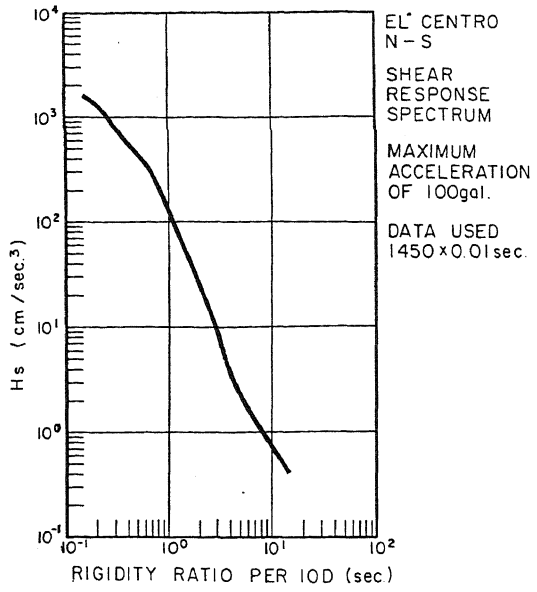

FIG.6 SHEAR RESPONSE SPECTRUM

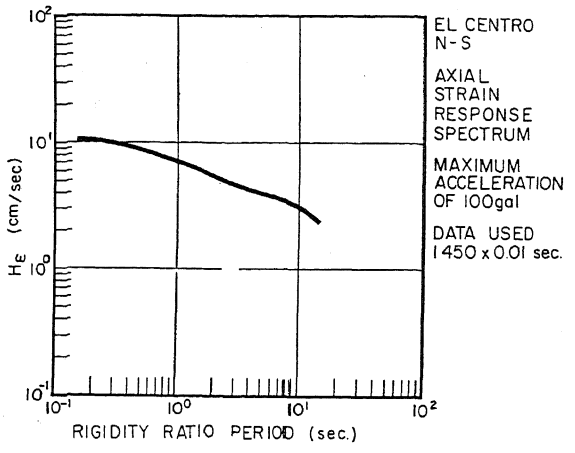

FIG.7 AXIAL STRAIN RESPONSE SPECTRUM

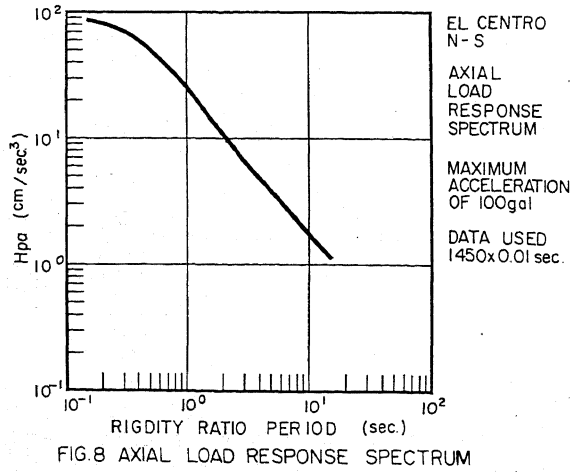

FIG.8 AXIAL LOAD RESPONSE SPECTRUM

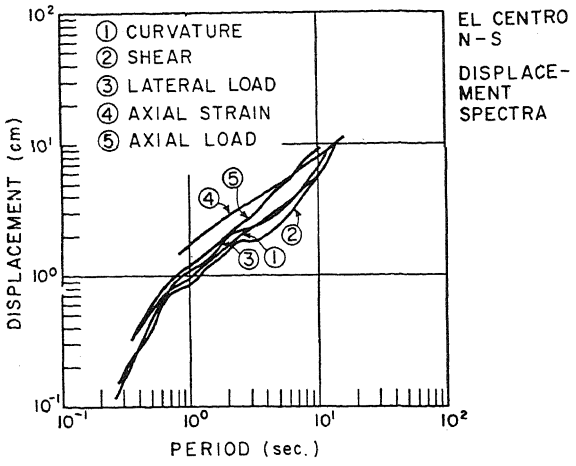

FIG.9 DISPLACEMENT SPECTRA

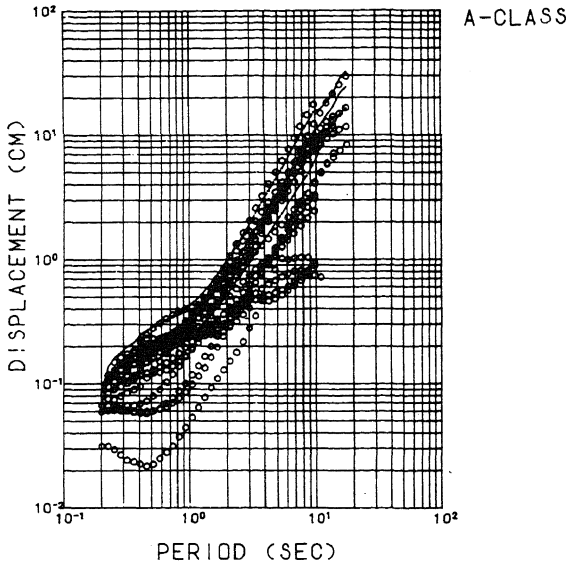

FIG.10 DISPLACEMENT SPECTRA FOR GROUP A

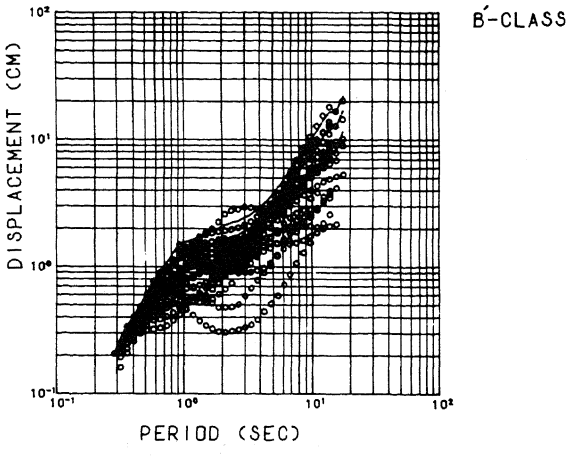

FIG.11 DISPLACEMENT SPECTRA FOR GROUP B'

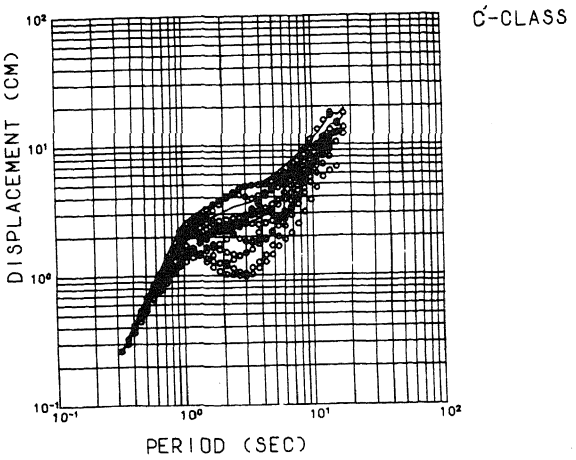

FIG.12 DISPLACEMENT SPECTRA FOR GROUP C'

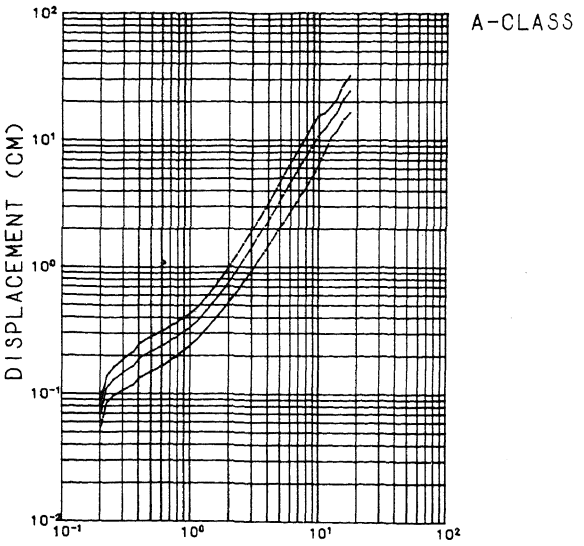

FIG.13 STANDARD SPECTRA FOR GROUP A

Group	Accelerogram			Classi-fication	Length	$\int \rho(\tau)$ cm/sec 2	Magunitude
A	Kushiro	S-369	E-W	A	1000	5.35	
	Miyako	S-236	N-S	A	2000	5.61	7.8
			E-W	A	2000	6.35	7.8
		S-271	N-S	A	1500	7.59	7.4
			E-W	A	1500	8.20	7.4
		S-273	N-S	A	1050	2.48	
			E-W	A	1050	3.03	
		S-312	N-S	A	2000	7.79	7.3
			E-W	A	2000	8.06	7.3
		S-420	N-S	A	1000	1.39	
			E-W	A	1000	5.60	
		S-537	N-S	A	1500	4.17	
			E-W	A	1500	4.92	
	Ofunado(B)	S-554	E-W	A	1050	8.87	6.2
	Kashima	S-196	N-S	A	1000	4.63	
			E-W	A	1000	6.40	
B	Muroran	S-234	N-S	C'	1800	26.0	7.8
			E-W	C'	1800	31.3	7.8
		S-241	N-S	B'	1500	10.5	7.4
			E-W	B'	1800	15.3	7.4
		S-399	N-S	B'	1500	10.8	6.9
	Hachinohe	S-252	N-S	C'	1500	30.8	7.8
			E-W	C'	1500	44.4	7.8
		S-310	N-S	B'	1800	19.8	7.3
			E-W	B'	1800	22.8	7.3
	Ofunado	S-140	E-W	B'	1500	26.9	
		S-282	N-S	C'	1800	45.9	?
			E-W	C'	1500	33.8	?
		S-361	N-S	B'	1500	25.4	
			E-W	B'	1500	25.4	
	Shinagawa	S-340	N-S	B'	1800	25.8	
			E-W	B'	1800	13.4	
	Kinuura	S-480	N-S	B'	1500	11.8	
			E-W	B'	1500	21.0	
	Hiroshima	S-364	N-S	B'	1500	16.0	
			E-W	B'	1500	29.7	
	Hososhima	S-213	N-S	C'	1500	30.7	7.5
			E-W	C'	1500	38.4	7.5
		S-453	N-S	B'	1500	15.8	
			E-W	B'	1500	9.8	
		S-544	N-S	B'	1800	23.5	6.7
			E-W	B'	1800	16.1	6.7
		S-545	E-W	B'	1000	10.5	6.1
C	Aomori	S-235	N-S	C'	2000	43.0	7.8
			E-W	C'	2000	50.5	7.8
		S-264	N-S	B'	2000	29.0	7.4
			E-W	B'	2000	27.1	7.4
	Kochi	S-211	N-S	C'	1800	51.0	7.5
			E-W	C'	1800	44.9	7.5

Table-1 Classified Strong-Motion Accelerograms

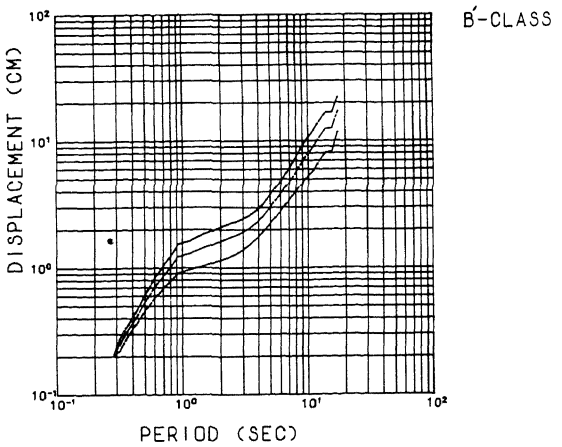

FIG.14 STANDARD SPECTRA FOR GROUP B'

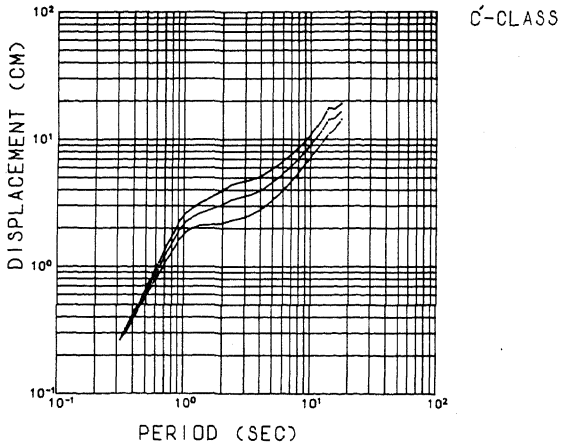

FIG.15 STANDARD SPECTRA FOR GROUP C'

ERRATA

"Spectra for Earthquake Resistive Design of Underground Long Structures

by Y. AOKI and S. HAYASHI

page	line	error	correction
561	8	repoduced	reproduced
561	31	upqards	upwards
563	27	apectra	spectra
567	Table-1	$H\rho(\tau)$	$H_\rho(\ 1\ )$